Journal of the Earth & Space Physics. Vol. 33, No. 3, 2008 1-12

2-D Euler de-convolution through DST of gravity data

Ardestani, E. V[1*].

[1]*Associate Professor, Earth Physics Department, Institute of Geophysics, University of Tehran and Center of Excellence in Survey Engineering and Disaster Management, Tehran, Iran*

(Received: 5 Dec 2005 , Accepted: 8 Sep 2007)

Abstract

The Different Similarity Transformation (DST) technique (Stavrev, 1997) utilizes a powerful and fully automatic tool for depth estimation of a point source through Euler de-convolution. Stavrev (1997) showed the results for the magnetic data of simple 2-D sources and aeromagnetic data along profiles. We apply the technique for the gravity data of 2-D rectangular models and real gravity data which has not been considered by Stavrev (1997).

Key words: Gravity, Depth estimation, Euler de-convolution

1 INTRODUCTION

The EULDPH method based on Euler's homogeneity of the anomalous fields has been defined and applied by Thompson (1982) and Reid et al (1990).

An important advantage of the method is that depth estimates can be obtained without any information about magnetization or density contrast of the source.

Klingele and Marson, (1991) and Marson and Klingele, (1993) used the method for gravity and gradiometric data.

They have shown that the accuracy of the results depends on the correct definition of structural index, sampling interval, decimation factor and moving interval of the window.

These dependencies make the method difficult to implement and it is fully subject to the interpreter.

Barbosa et al. (1999) proposed some modifications to Euler de-convolution for structural index estimation of magnetic data through stability analysis.

Stavrev (1981) expressed the concept of similarity transformations. The differences between the transformed and the original data form differential similarity transformations (DSTs).

Stavrev (1997) used the DST approach for a joint optimum estimation of the structural index and the coordinates of a one-point source. The results of applying DST for magnetic data of simple sources and aeromagnetic data were presented by Stavrev (1997).

2 DST

The Euler de-convolution of one-point source anomalies using DST is described by Stavrev (1997).

For estimating the coordinates of a point source and structural index, the following system of normal equations must be solved,

$$\sum_i t_{ij} p_j = r_i \qquad i = 1,2,3, \qquad j = 1,2,3 \tag{1}$$

where $p_1 = a, \quad p_2 = c, \quad p_3 = -N$ and a and c are the coordinates of central point of similarity and N represents the structural index (Thompson, 1982).

$$t_{ij} = \sum_m E_m[D_j]\ E_m[D_i], \qquad m = 1,2,....,K \tag{2}$$

$$r_i = \sum_m G_m E_m[D_i], \tag{3}$$

$$G_m = E_m[xD_1] + E_m[zD_2], \tag{4}$$

$$D_1 = \frac{\partial F}{\partial x}, \quad D_2 = \frac{\partial F}{\partial z}, \quad D_3 = F, \tag{5}$$

$$E_m[H] = H_m - H_0 - q[H\}Ro, \tag{6}$$

$$H_m = H(x_m, z_m), \tag{7}$$

$$H_0 = \sum_\omega H_\omega / K, \tag{8}$$

[*]Corresponding author: Tel: 021-61118206 Fax: 021-88630548 E-mail: ebrahimz@ut.ac.ir

$$q_v[H] = \sum_{\omega}(v_\omega - v_c)(H_\omega - H_0)/ \sum_{\omega}(v_\omega - v_c)^2, \quad \omega = 1,2,...,K, \tag{9}$$

where v=x, z, i.e. coordinates of the observation points p, K is the number of observation points, $v_c = x_c, z_c$ i.e. coordinates of the window central point Oc, and H is a common symbol of the functions on which the operator E is exercised.

Ro is the distance vector of the observation point to the central point of the window.

The solution of (1) gives optimal values of the coordinates x_0, z_0 of the singular point M, the structural index N and the coefficients of the background trend,

$$x_0 = p_1, \; z_0 = p_2, \; N = -p_3, \tag{10}$$

$$b_v = q_v/(p_3 - 1), \quad v = x, z \tag{11}$$

$$B_0(x_c, z_c) = \{S_0 - (p_1 - x_c)b_x - (p_2 - z_c) b_z\}/p_3, \tag{12}$$

where

$$q_v = \sum_m \{(v_m - v_c)(S_m - S_0)\}/\sum_m (v_m - v_c)^2, \quad m = 1,2,....,K, \tag{13}$$

$$S_m = p_3 F_m - (x_m - p_1)(D_1)_m - (z_m - p_2)(D_2)_m, \tag{14}$$

$$S_0 = \sum_{\omega} S_\omega / K, \quad \omega = 1,2,...,K. \tag{15}$$

The quality and the dispersion of the solution can also tested through relevant equations (Stavrev, equations (35), (36), 1997),

$$Qm^2 = \sum_m \{S_m - S_0 - (x_m - x_0)q_x - (z_m - z_c) q_z\}^2/(K - U_c), \; m = 1,2,...,K, \tag{16}$$

where Qm is the minimum of the object function (Stavrev, equations (30), 1997) and reflect the quality of the solutions.

The dispersions of the solutions of system (1) are determined by,

$$\sigma_i^2 = d_{ii} Q_m^2 (K - U_c)/(K - U), \quad i = 1,2,3, \tag{17}$$

where d_{ii} are the diagonal elements of the inverse matrix of the coefficients t_{ij} in (1), U is the number of unknowns (U=3), K is the number of points in the window.

3 NUMERICAL PROCEDURES

To implement the DST technique for a point source anomaly the following procedure is applied.

1. Computing the gravity anomaly of synthetic models through Talwani's (1959) method along the profile and in definite x points or considering a profile passing through the center of anomaly in the case of real data.
2. Computing the interpolated values of gravity data along the profile, using cubic spline method (Press et al., 1986).
3. Substituting $\frac{\partial g}{\partial z}$ instead of F in equation (5) (Klingele and Marson, 1991) yields,

$$D_1 = \frac{\partial^2 g}{\partial x \partial z}, \quad D_2 = \frac{\partial^2 g}{\partial z^2}, \quad D_3 = \frac{\partial g}{\partial z}, 8) \tag{18}$$

4. Constructing the linear system of equations by considering equation (9),

$$q[H]Ro = \left(\frac{\sum_{\omega}(x_\omega - x_c)(H_\omega - H_0)}{\sum_{\omega}(x_\omega - x_c)^2} \right) (Xop) + \left(\frac{\sum_{\omega}(z_\omega - z_c)(H_\omega - H_0)}{\sum_{\omega}(z_\omega - z_c)^2} \right) (Zop), \omega = 1,2,...,K \tag{19}$$

where Xop and Zop are the distances of the observation points to the window central point in x and z directions, respectively.

Substituting equation (7), (8) and (17) into equation (6), the elements of the t_{ij}, (3*3) matrix are constructed following equation (2).

$$\sum_{m=1}^{K} E_m[D_1]E_m[D_1] \quad \text{when} \quad i=1, \quad j=1, \tag{20}$$

$$\sum_{m=1}^{K} E_m[D_1]E_m[D_2] \quad \text{when} \quad i=1, \quad j=2, \tag{21}$$

$$\sum_{m=1}^{K} E_m[D_1]E_m[D_3] \quad \text{when} \quad i=1, \quad j=3, \tag{22}$$

$$\sum_{m=1}^{K} E_m[D_2]E_m[D_1] \quad \text{when} \quad i=2, \quad j=1, \tag{23}$$

$$\sum_{m=1}^{K} E_m[D_2]E_m[D_2] \quad \text{when} \quad i=2, \quad j=2, \tag{24}$$

$$\sum_{m=1}^{K} E_m[D_2]E_m[D_3] \quad \text{when} \quad i=2, \quad j=3, \tag{25}$$

$$\sum_{m=1}^{K} E_m[D_3]E_m[D_1] \quad \text{when} \quad i=3, \quad j=1, \tag{26}$$

$$\sum_{m=1}^{K} E_m[D_3]E_m[D_2] \quad \text{when} \quad i=3, \quad j=2, \tag{27}$$

$$\sum_{m=1}^{K} E_m[D_3]E_m[D_{31}] \quad \text{when} \quad i=3, \quad j=3, \tag{28}$$

Keeping in mind equation (4) for G_m the elements of r_j vector are computed through equation (3).

5. Solving the system of normal equations (1) by the least-square approach,

$$\bar{x} = (A^T A)^{-1} A^T d \tag{29}$$

where A represent the matrix (equation, 20-28).

6. Calculating the condition number of $A^T A$ (Press et al., (1986)) to evaluate the condition of this matrix during its inversion. Although this number has no application in computations.
7. Computing the quality of the solutions by equation (16).
8. Computing the dispersion of the solutions by equation (17). This criterion enables us to define an acceptance level for the solutions.

4 SYNTHETIC MODELS

The DST technique is used for the depth estimation of the simple 2-D rectangular models. The window size is chosen to be greater than the depth of the source under estimation considering the recommendation of Stavrev (1997). At this step for distinguishing the best factors for selecting the suitable results we used noise free data without noise.

The window should include a sufficient number of points (more than 7).

The results of implementing the technique for simple rectangular shapes with a contrast density equal to 1 g/cm^3 are shown in tables. (1-6).

Some results are presented in the tables.

Table 1. Win. Size.=12 dec.=1. dnemo=1.m.

No	Xeuler (m)	Depth (m)	Con.No.	Q
1	26.36	-1.13	3.15	0.079
2	26.55	-1.69	3.09	0.038
3	26.73	-1.99	3.02	0.013
4	27.62	0.0366	2.92	0.063
5	30.92	5.94	2.151	0.28
6	34.86	3.25	0.49	0.19

In this table the depths No. (4), (5) and (6) are positive and could be the right depths.

Table 2. Win. Size.=12 dec.=1. dnemo=1.3m.

No.	Xeuler (m)	Depth (m)	Con.No.	Q
1	19.23	-4.208	2.97	0.25
2	19.66	-1.62	2.95	0.018
3	22.81	6.95	2.91	0.76
4	28.95	12.3	2.55	1.86
5	35.39	6.23	0.7	0.94
6	39.22	-3.58	0.95	0.077
7	39.16	-6.64	2.52	0.312
8	38.03	-5.65	3.05	0.76
9	36.66	-2.82	3.26	1.14
10	36.97	-1.64	3.3	1.2

In this table the depths No.(3)-(5) are positive and could be the right ones.

Table 3. Win. Size.=12 dec.=1. dnemo=1.3m.

No.	Xeuler (m)	Depth (m)	Con.No.	Q
1	22.56	-2.28	3.08	0.6
2	22.47	-2.83	3.06	0.42
3	21.99	-3.73	3.0	0.142
4	22.77	0.9	2.95	0.07
5	26.99	9.17	2.88	0.73
6	33.62	10.88	1.195	1.03
7	39.64	2.168	0.62	0.294
8	42.2	-5.71	1.04	0.077
9	41.31	-6.47	2.54	0.425
10	40.59	-4.61	3.17	0.67

In this table the depths No.(4)-(7) are positive and could be the right ones.

Table 4. Win. Size.=12 dec.=1. dnemo=0.85m.

No.	Xeuler (m)	Depth (m)	Con.No.	Q
1	24.57	-1.04	3.12	0.093
2	23.89	-2.21	3.0	0.093
3	24.07	-1.77	2.96	0.028
4	25.23	1.99	2.91	0.0097
5	28.33	6.6	2.66	0.15
6	32.03	4.78	0.66	0.48
7	34.84	-1.34	0.62	0.38
8	35.31	-3.99	1.4	0.073
9	35.13	-3.57	2.65	0.028
10	34.37	-2.1	3.25	0.076

In this table the depths No.(4)-(6) are positive and could be the right ones.

Table 5. Win. Size.=12 dec.=1. dnemo=1.0m.

No.	Xeuler (m)	Depth (m)	Con. No.	Q
1	33.86	2.96	3.96	1.8
2	35.74	4.51	2.8	2.008
3	36.59	19.93	2.7	5.81
4	32.4	10.75	2.7	1.36
5	28.23	12.8	2.81	3.57
6	31.7	15.11	2.81	9.14
7	35.65	13.6	2.8	11.82

In this table all the depths are positive.

Table 6. Win. Size.=12 dec.=1. dnemo=1.0m.

No.	Xeuler (m)	Depth (m)	Con.No.	Q
1	24.17	6.5	2.93	0.93
2	29.93	11.97	2.5	2.24
3	36.7	6.08	0.6	1.16
4	40.45	-3.11	0.8	0.122
5	28.33	6.6	2.66	0.15
6	32.03	4.78	0.66	0.48
7	34.84	-1.34	0.62	0.38
8	35.31	-3.99	1.4	0.073
9	35.13	-3.57	2.65	0.028
10	34.37	-2.1	3.25	0.076

In this table depths No. (1)-(3), (5) and (6) are positive. In these tables win.size is the number of points of the window, dec. is the interval between two operator points (decimation factor), Con.No. is the condition number of matrix, Q is the quality of the solution and dnemo is the distance of interpolation of original data which have been calculated through the Talwani et al. (1959) method and 5m grid spacing. The admissible standard deviation of N is less than |0.25| and according to Stavrev (equation (51), 1997) for a two-dimensional point source, the structural index (N) satisfies the following criterion, $-0.5 < N < 2.5$.

Considering the positive depths (tables 1-6), the depths in the place where Xeuler is the closest to the center of the anomaly are the best ones (figures 1-6). Other factors like Con. No. and Q are not usually useful for selecting the best results.

5 FIELD EXAMPLES

The set of real data used for testing the DST technique were recorded at the Institute of Geophysics and at the Institute of Petroleum Engineering Department, University of Tehran. To recognize and to delimit the subsurface water tunnel (ghanat), a microgravity survey based on two parallel profiles was measured at the Institute of Geophysics.

A CG3M gravimeter is used to collect the data. The station separation of 2 m was chosen. The residual anomalies are shown in figure 7 The DST technique is applied to estimate the depth of the tunnel along one of the main profiles (X=6 m and y from 2 to 14 m) and the results are shown in table 7.

In this table the depths No. (1)-(3) are positive and number (2) is the closest one to the center of the anomaly. Observing the depth of the ghanat in the neighbor well in the area, the depth of the tunnel must be something between 3 and 5

meters.
The closest Xeuler to the center of the anomaly is plotted in figure 8 which represent the depth very accurately.

Another survey has been conducted on the foundation of the Institute of Petroleum Engineering Department to detect the probable old ghanat or surplus water wells.

The station separation is again 2 meters. The residual anomalies are shown in figure 9.

The results of DST technique along the profile Y=12 m are shown in table 8.

Table 7. Win. Size.=12 dec.=1. dnemo=0.5m.

No.	Yeuler (m)	Depth (m)	Con. No.	Q
1	4.64	2.67	1.5	1.5e-7
2	5.37	4.5	2.9	4.2e-7
3	5.16	1.9	0.6	3.35e-7
4	8.68	-2	3.35	5.2e-7

Table 8. Win. Size.=12 dec.=1. dnemo=0.8m.

No.	Xeuler (m)	Depth (m)	Con. No.	Q	σ^2
1	14.96	2.94	2.4	2.6e-3	1.23e-4
2	14.13	4.69	0.7	3.47e-3	1.34e-4
3	13.99	5.08	0.9	3.31e-3	1.26e-4
4	13.72	4.6	1.06	3.44e-3	2.3e-4
5	13.04	2.6	0.6	2.42e-3	1.5e-4

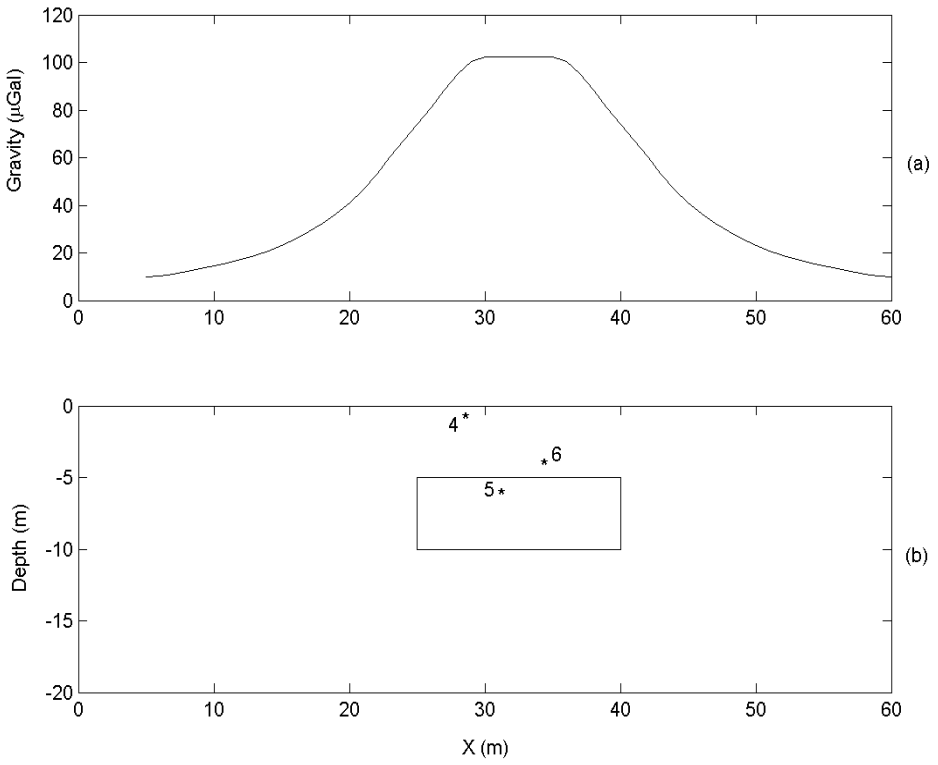

Figure 1. (a) The gravity effect of the block. (b) The rectangular block and DST source points X=25-40 meters, Z=5-10 meters.

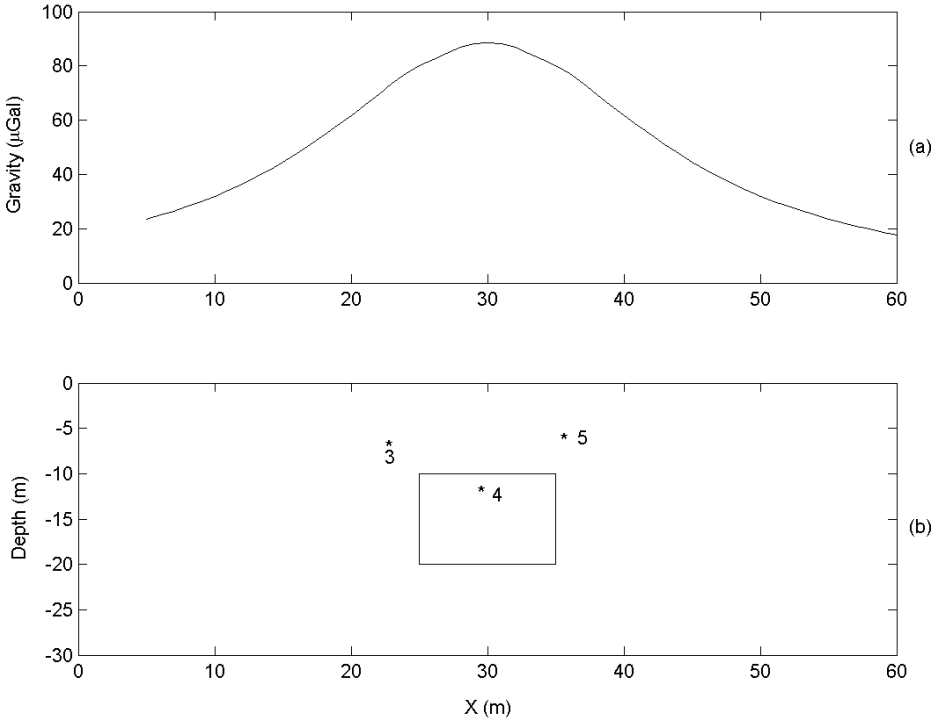

Figure 2. (a) The gravity effect of the block. (b) The rectangular block and DST source points X=25-35 meters, Z=10-20 meters.

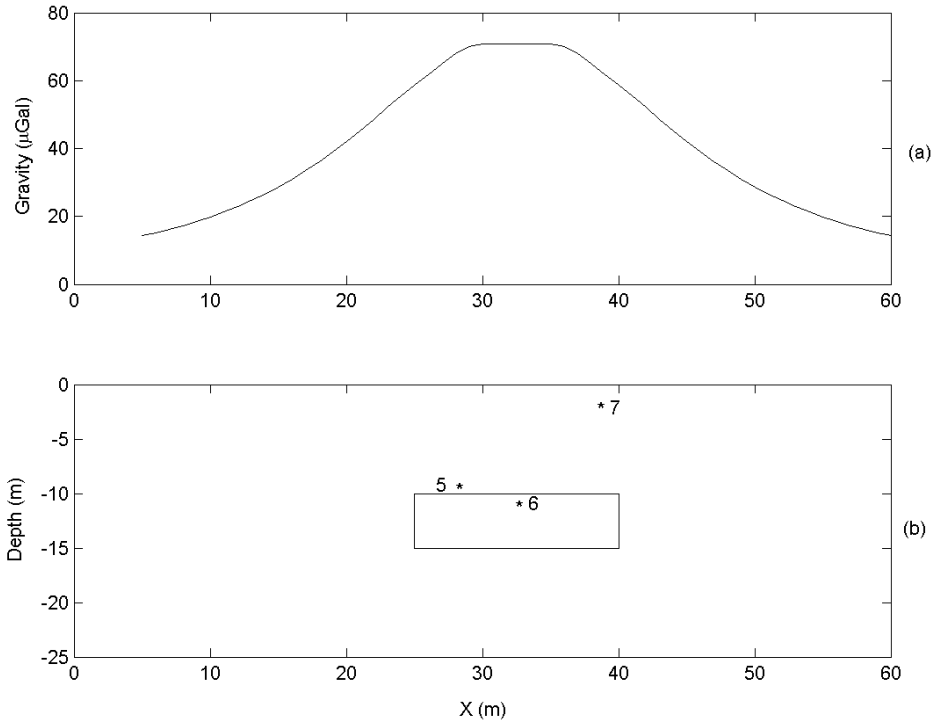

Figure 3. (a) The gravity effect of the block. (b) The rectangular block and DST source points X=25-40 meters, Z=10-15 meters.

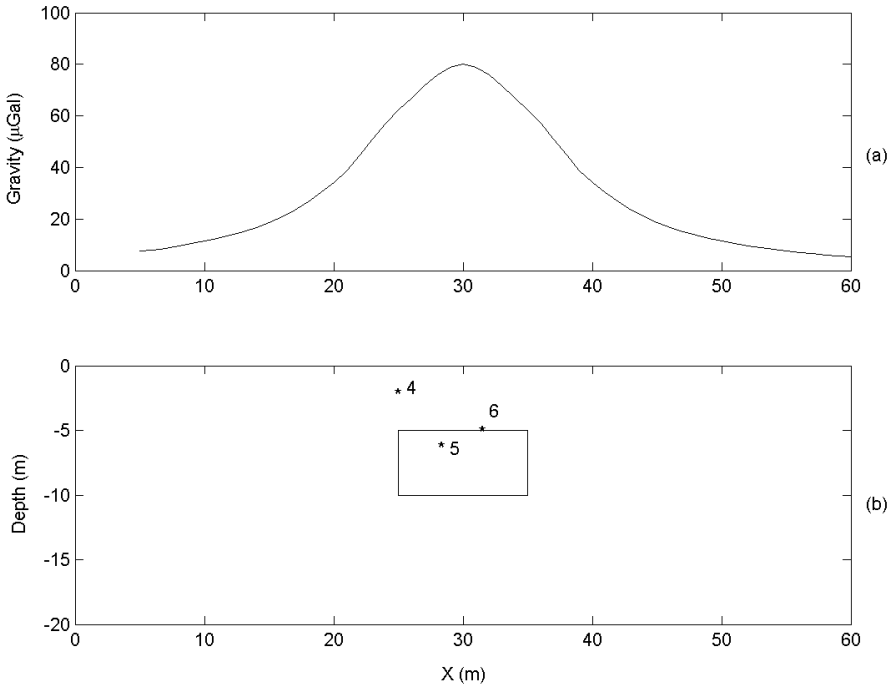

Figure 4. (a) The gravity effect of the block. (b) The rectangular block and DST source points X=25-35 meters, Z=5-10 meters.

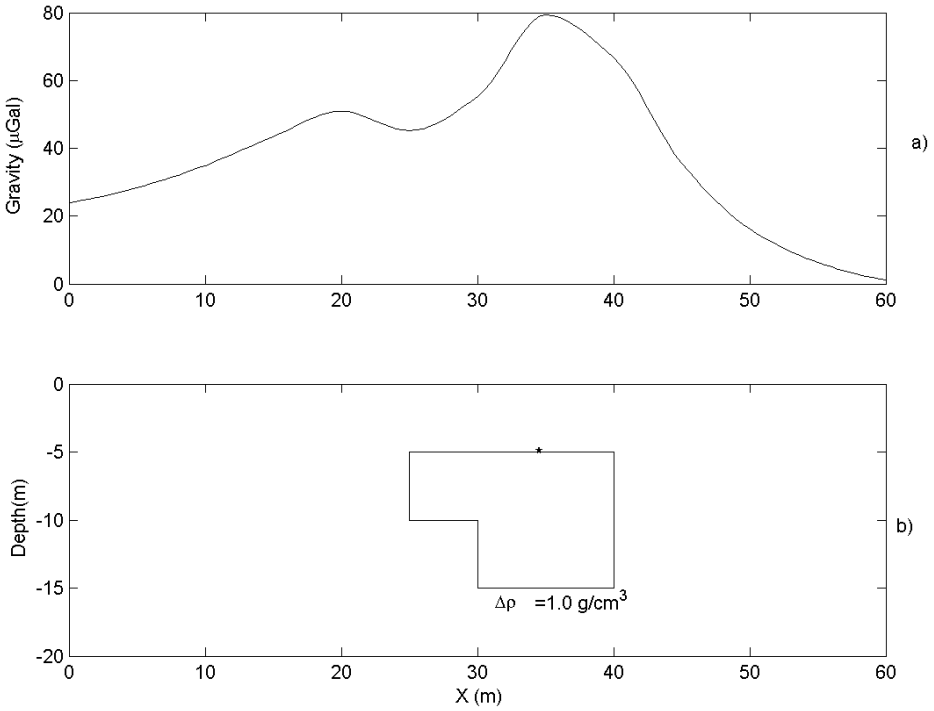

Figure 5. (a) The gravity effect of the block. (b) The rectangular block and DST source points X=25-40 meters, Z=5-15 meters.

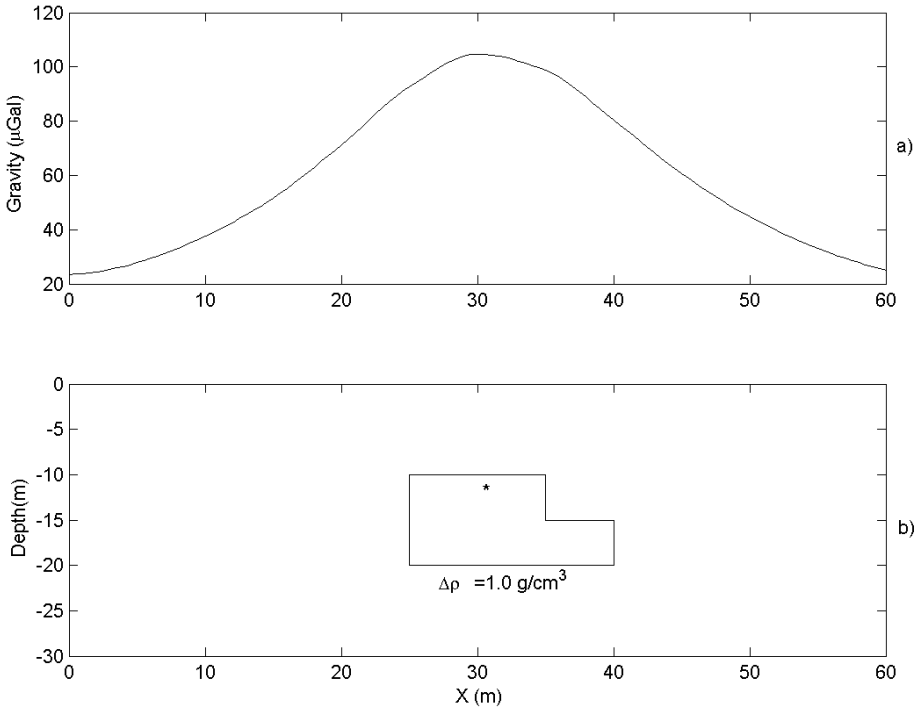

Figure 6. (a) The gravity effect of the block. (b) The rectangular block and DST source points X=25-40 meters, Z=10-20 meters.

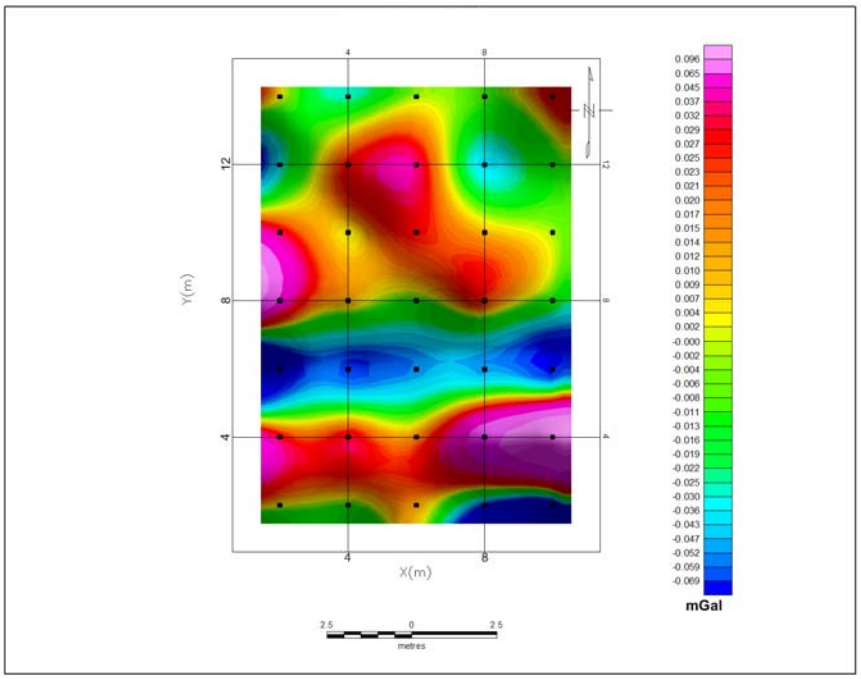

Figure 7. The residual anomaly map (mGal).

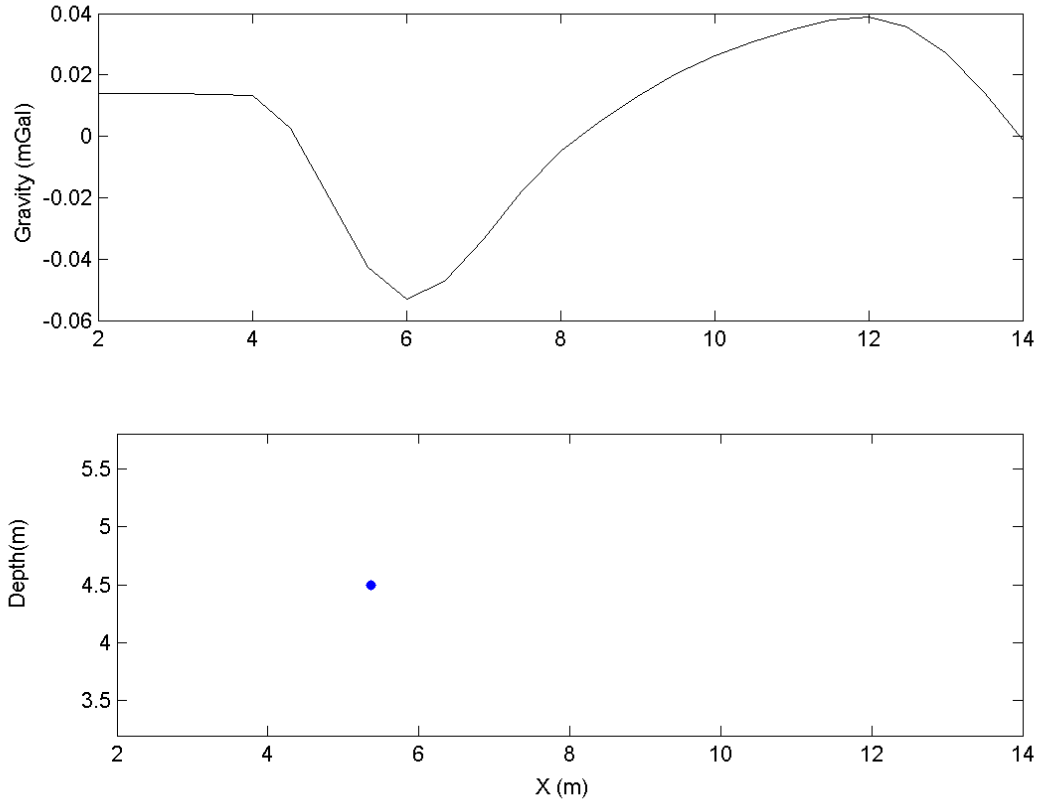

Figure 8. (a) The residual gravity anomaly along the first profile. (b) The DST point sources.

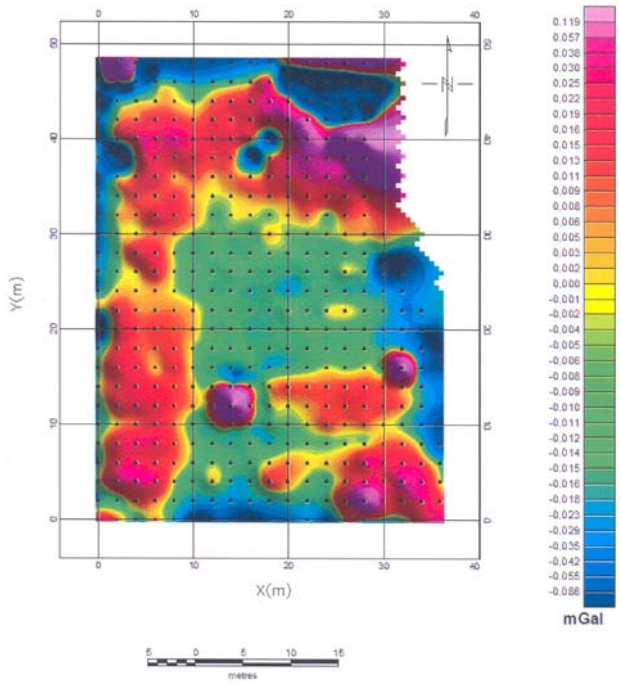

Figure 9. The residual anomaly map (mGal).

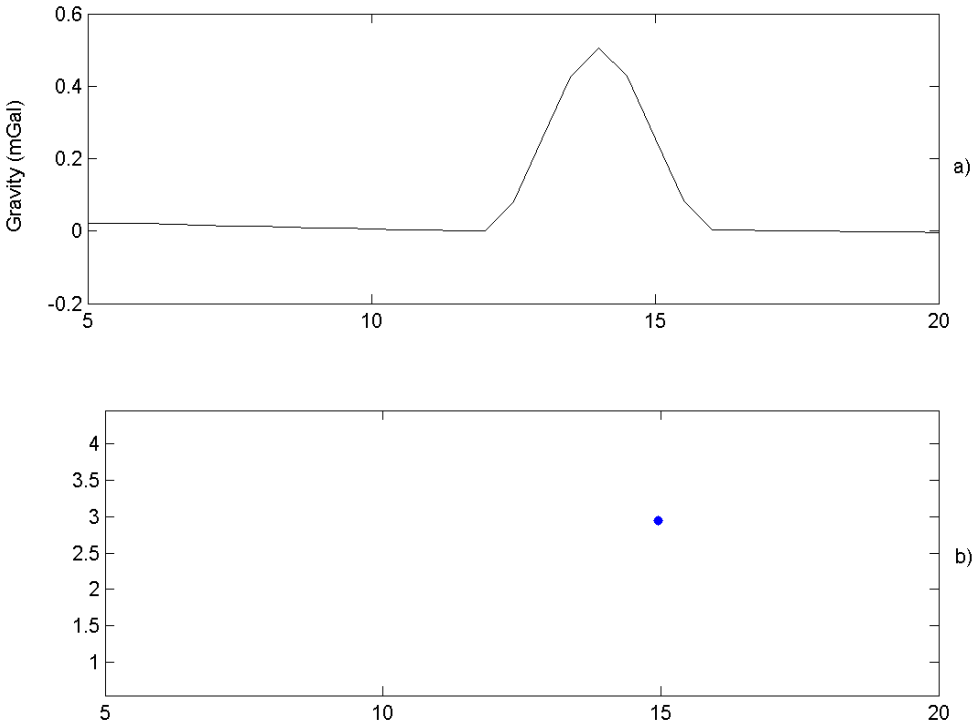

Figure 10. (a) The residual gravity anomaly along the second profile. (b) The DST point sources.

In this table all the depths are positive. Number (5) has the smallest value of Con. No. and Q but is not close to the center of the anomaly. Based on our experience in synthetic models No. (1) which is the closest point to the center of the anomaly could be the result if although its Con. No. is the largest. The depth of upper surface of the surplus water well is also determined after excavation about 2.5 meters.

The closest Xeuler to the center of the anomaly is plotted in figure 10.

4 CONCLUSIONS

The DST technique is quite effective and flexible for estimating the depth of gravity sources. The automatic determination of the structural index is a main advantage.

Meanwhile different shapes of the sources and decimation factors or position of the windows do not affect the results. Inspecting the solutions, a small number of them are acceptable that decrease the role of the interpreter's judgment. However, the technique gives relatively precise results in the middle of the anomaly where the anomaly peaks. In the case of the complex anomalies only the depth under the highest peak of the anomalies is accurate. Some criteria for the accuracy of the solution defined by Stavrov (1997) such as dispersion (σ^{2}), object function (Q) or condition umber are not so useful for highlighting the best solution.

ACKNOWLEDGEMENTS

The author is thankful to the Institute of Geophysics, University of Tehran, and Eng. V. Sharbaf for assistance in providing the data.

REFERENCES

Barbosa, C. F., Silva, J. B., and Medeiros, W. E., 1999, Stability analysis and improvment of structural index estimation in Euler deconvolution. Geophysics, **64**, 48-60.

Klingele, E. E., and Marson, I., 1991, Automatic interpretation of gravity gradient data in two dimension: Vertical gradient. Geophys. Prospect., **39**, 407-439.

Marson, I., and Klingele, E. E., 1993, Advantages of using the vertical gradient of gravity for 3-D interpretation. Geophysics, **58**, 1588-1595.

Press, W. H., Teukolsky, S. A., Vetterling, W. T., and Flannery, B. P., 1986, Numerical recipes in Fortran. Cambridge University Press.

Reid, A. B., Allsop, J. M., Granser, H., Millet, A. J., and Somerton, I. W., 1990, Magnetic interpretation in three dimensions using Euler de-convolution. Geophysics, **37**, 1043-1045.

Stavrev, P. Y., 1981, Similarity transformations of gravity and magnetic anomalies. Bulgarian Geophys., J. **VII(3)**, 95-106.

Stavrev, P. Y., 1997, Euler de-convolution using differential similarity transformations of gravity or magnetic anomalies. Geophys. Prospect., **45**, 207-246.

Talwani, M., Worzel J. L., and Landisman, M., 1959, Rapid gravity computation for two-dimensional bodies with application to the Mendocino submarine fracture zone. J. Geophys. Res., **64**, 49-59.

Thompson, D. T., 1982, EULDPH, A new technique for making computer-assisted depth estimates from magnetic data, Geophysics, **47**, 31-37.